

1. Technical Introduction

In their investigations, the brothers Pierre & Jacques Curie found that electrical charges were produced by mechanical stresses applied to various naturally occurring crystals. This phenomenon is called the 'piezo-electric effect', being derived from the Greek word 'to press'.

Conversely it was found that the crystal was deformed by the application of an electrical charge, later the application of an alternating electrical field introduced mechanical vibrations.

The quartz crystal behaves as an electrical resonance circuit with very low attenuation.

2. Quartz

Quartz was found to be one of the naturally occurring crystalline substance that exhibited the 'piezo-electric effect' and being very stable, both chemically and mechanically, it became of great interest to the early electronic experimenters. The chemical description of Quartz is Silicon dioxide SiO_2 .

Although approximately 14% of the earth's crust consists of SiO_2 , it occurs relatively infrequently in usable crystalline form with the necessary purity and without physical defects, cracks etc. Raw quartz of quality suitable for the production of quartz crystal units is found in Brazil and Madagascar.

For this reason continuous attempts have been made to produce quartz synthetically; that is to grow by recrystallisation on to quartz seed plates. These processes are now commercially successful.

Quartz chippings are dissolved in an alkaline solution in steel autoclaves at approximately 400°C and a pressure of 10.000 N/cm^2 , the desired direction of growth is ensured by the careful pre-orientation of the quartz seed plates.

The growth rate is normally approximately 1 mm/day. Slow growth-rates result in a more homogeneous material since fewer foreign atoms are being incorporated into the crystal lattice.

Synthetic quartz is now grown in suitable length and cross sections to enable the subsequent processing steps to be carried out in the most efficient way, with minimum cutting losses. Grades available today are of very high purity and mechanical quality, so that synthetic quartz is used almost exclusively for the production of quartz crystal units.

3. AT-cut

Its outstanding physical properties have made the AT-cut the most used cut for oscillator crystal production. The position of the AT-cut relative to the crystal axis can be seen from the marginal schematic presentation of a half quartz crystal (Fig. 1).

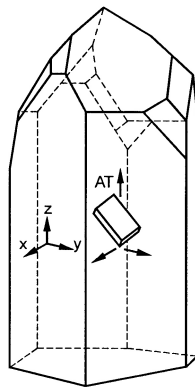


Fig. 1: Position of the AT-Cut relative to the crystal axis

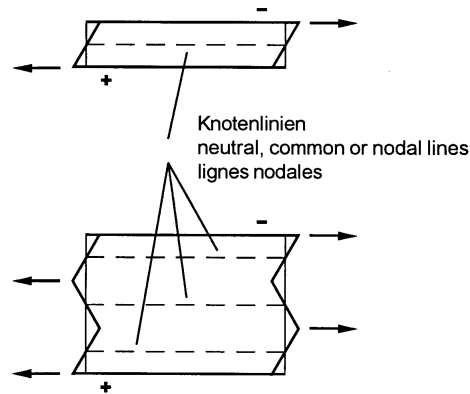


Fig. 2: Polarity Diagram

Usually, oscillator crystals in the AT-cut are manufactured in the frequency range 800 kHz to 360 MHz, from 800 kHz to 40 MHz in fundamental mode and from 10 MHz to 360 MHz overtone mode oscillations are employed.

AT-cut crystals are thickness shear vibrators. The crystal vibrator is usually a round disc. The thickness (d) of the disc is related to the fundamental mode frequency f by the equation:

$$f[\text{kHz}] = \frac{N}{d[\text{mm}]}$$

The constant for the AT-cut is $N = 1660 \text{ kHz} \cdot \text{mm}$.

The crystal vibrator has thin metal electrodes deposited on both sides by evaporation, these electrodes are the means whereby the alternating electric field is applied thus stimulating the mechanical oscillation. With overtone oscillation, only odd-numbered harmonics can be generated, as can be seen from the polarity diagram (Fig. 2). With an even-numbered over-tone, the electrodes would show identical polarity and consequently no electric field will develop for the stimulation of mechanical oscillation.

Normal overtone oscillations are the 3rd, 5th, 7th and 9th, the upper harmonic oscillation is not exactly an integral multiple of the crystal fundamental frequency but can differ from this up to some percents. The principal advantage of AT-cut over other cuts is the low frequency sensitivity to change in temperature, it follows a 3rd degree curve (Fig. 3), a so-called "cubical parabola" with an inflection point which lies between 25° and 35°C depending on the actual cut angle and mechanical construction.

$$\frac{\Delta f}{f} = A_1 \cdot (T - T_{ref}) + A_2 \cdot (T - T_{ref})^2 + A_3 \cdot (T - T_{ref})^3$$

This equation can be reduced, if one refers to the inflection point temperature T_{inv} instead of the initial temperature T_{ref} .

$$\frac{\Delta f}{f} = A_1 \cdot (T - T_{inv}) + a_3 \cdot (T - T_{inv})^3$$

$$\text{whereby } a_3 = 1,05 \cdot 10^{-4}$$

$$a_1 = -0,085 \cdot \Delta\varphi$$

$$\Delta\varphi = \varphi_{zz} - \varphi_0 \quad \text{in one - sixtieth of one angular degree}$$

$$\frac{\Delta f}{f} \quad \text{in ppm} \left[= 10^{-6} \right] \quad \text{and temperatures in } ^\circ\text{C}$$

The steepness at the inversion point depends on the angle of cut is the difference in cut angle between the so called zero angle where the temperature curve has a horizontal tangent at the inflection point.

By the choice of the appropriate cutting angle, two inversion points appear in the temperature curve, a maximum below 25°C and a minimum above this temperature. At each of these inversion points the temperature gradient is zero.

This property is, at the upper inversion point, utilised where crystals are operating in a thermostatically controlled environment (oven), judicious choice of the cutting angle will cause the zero temperature gradient point to coincide with the thermostat temperature, thus the thermostat or oven temperature must be clearly stated when ordering crystals for this particular use.

From Fig. 3 it can be seen that symmetrical ranges of temperature with respect to the inflection point, e.g. - 20°C to + 70°C or 0° to + 50°C are meaning full. A one-sided limitation, such as e.g. at 0° to + 70°C means no relief for the manufacturer in general, due to the symmetry of the curves the suggested tolerance – in our case down to - 20°C – is only observed with opposite (plus or minus) signs.

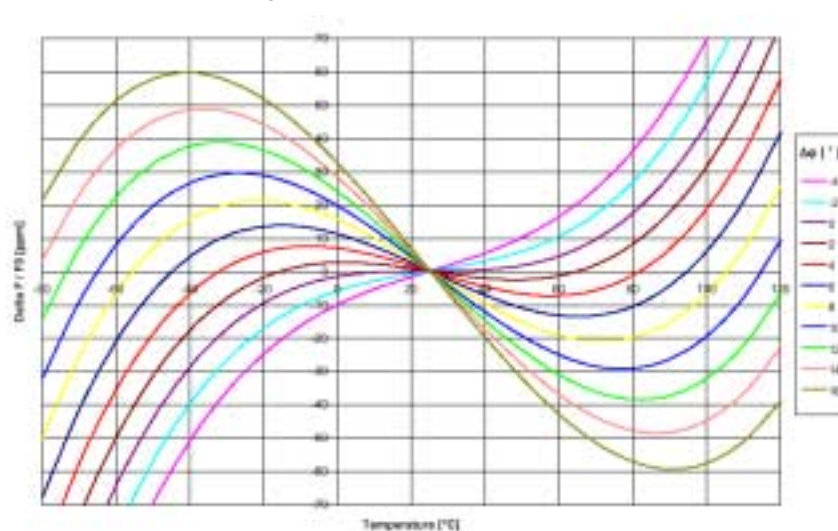


Fig. 3: Temperature Characteristics

Cutting angles of approximately 10 arc seconds can be accurately maintained, however other mechanical effects can influence the variation of frequency over the temperature range, thus technical as well as physical limitations are imposed on minimizing the temperature coefficient.

Figure 4 shows the possible frequency stabilities over temperature ranges and the respective difficulty level.

The graphs

- are valid for plane parallel fundamental crystals and overtone crystals.
- only serve as an indicator according to (DIN) IEC 122-1 Fig. 20 „AT cut crystal units – frequency tolerance/temperature range difficulty aspect.“.

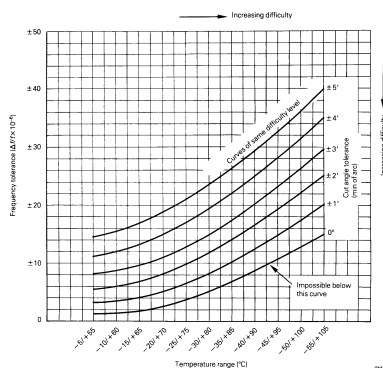


Fig. 4: Frequency Stability Over Temperature

For the determination of the frequency temperature coefficient it is sufficient – for simple requirements – to measure the frequencies at three temperatures. For higher accuracy, five measuring points or more may be necessary. By means of these, the best adapted cubical parabola is applied and the appropriate coefficients a_1 , and a_3 determined.

A correctly designed resonator should produce a smooth curve for its temperature coefficient with the value of a_3 within $\pm 20\%$ of the value indicated above. In the case of other temperature ranges, the accuracy of the temperature (TK) curve can be increased by adding a 4th-order term in the equation on page 2.

Resistance dips in the temperature range, also called activity perturbations, are caused by the hazardous stimulation of the quartz crystal modes.

As the vibrational modes have different temperature coefficients it might happen that other vibrational modes such as flexural vibration, extension vibration and face shear vibration, etc. or multiples of the fundamental frequency (Fig. 6) may coincide in the temperature range with the AT-cut.

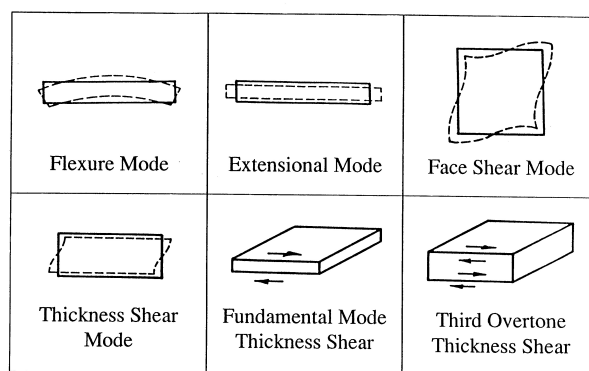


Fig. 6: Vibrational Modes

By means of this coupling with unwanted modes, energy is taken from the usable frequency vibration and results in damping. This becomes noticeable in a resistance dip (R1 increase) and in a frequency jump (Fig. 7).

Already existing dips are appearing significantly in the case of increased drive level. The optimum drive level in order to avoid or reduce the dips is in the range of 10 μ W to 100 μ W. For most of the other quartz crystal parameters the optimum drive level is between 10 μ W to 100 μ W which is recommended by TQ.

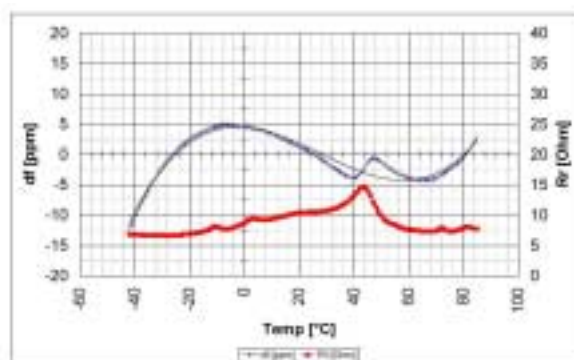


Fig. 7: Resistance Dip

Thermometric quartz crystals have a very strong temperature dependence of the resonance frequency. The characteristic of the thermometric quartz crystal, designated QT cut by TQ, is approximately linear in the temperature range -40°C to $+150^{\circ}\text{C}$. The linear coefficient is dependent on design and can be specified as typically 90 ppm/K. The square-law coefficient is 0.08 ppm/K².

Enclosure type HC-52/U is used owing to the low thermal time constant.

4. DRAT-Crystals

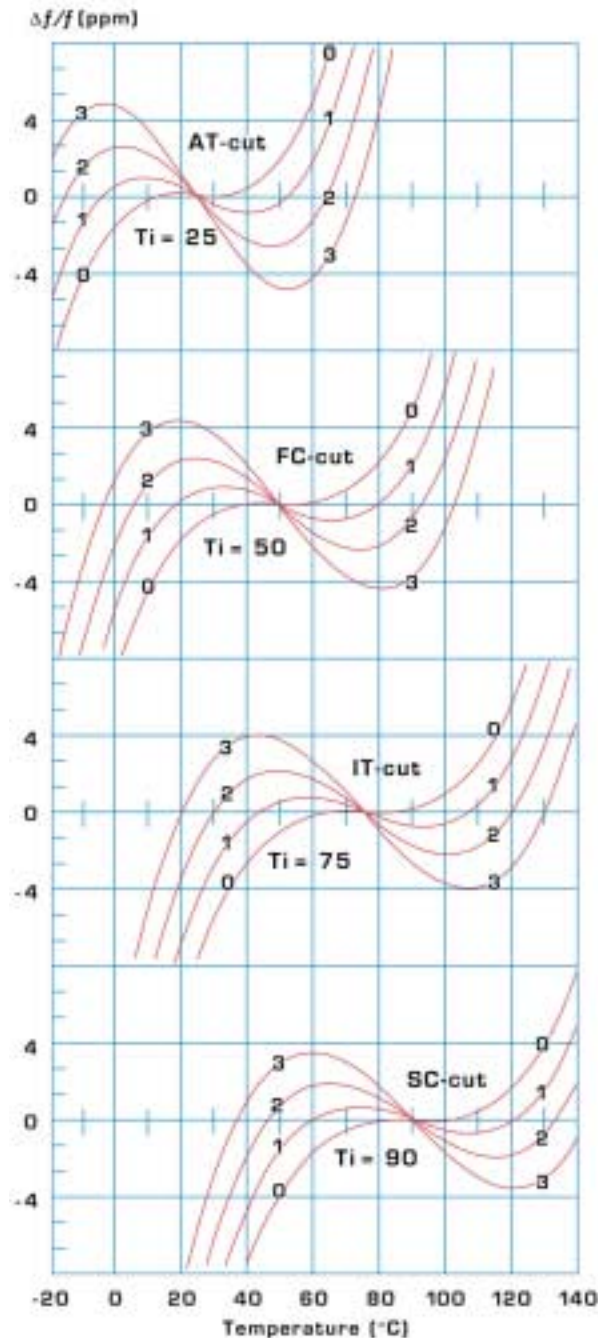


Fig. 8: Doubly rotated crystal resonators

Doubly rotated crystal resonators such as FC-cut, IT-cut and SC-cut crystals have significantly different operating characteristics than the popular AT-cuts and can provide some performance advantages in certain applications.

The frequency-temperature curves of DRAT resonators are very similar to those of AT-cuts and the major difference is the inflection temperature (T_i) (Fig. 8). This is the temperature at which the second derivative of the frequency-temperature curve becomes zero and is typically in the area of 25°C to 30°C for AT-cuts depending on design and frequency. The inflection temperature for DRAT cuts is in the area of 45°C to 55°C for FC-cuts, 70°C to 80°C for IT-cuts and 85°C to 95°C for SC-cut. Curves of DRAT resonators are also flatter than corresponding AT-cuts.

The temperature stability advantage is valid only for higher temperatures where DRAT resonators can show up to 10 times improvement in stability over their AT counterparts. For wide temperature ranges which include temperatures below 0°C, better stability can be obtained with AT-cut resonators.

The main advantages of these resonators, and in particular the SC (Stress Compensated) type, are:

- improved frequency-temperature stability for ovenized applications with operating temperatures in the 60°C to 100°C temperature range
- reduced amplitude frequency effect which allows higher drive levels and improved signal to noise ratio
- superior thermal transient characteristics resulting in improved short term stability and faster warm up times in oven operation
- improved aging characteristics
- improved vibration sensitivity (up to 2-3 times better than equivalent AT-cut resonators)
- higher C_0/C_1 ratio resulting in reduced sensitivity to circuit component changes
- higher Q-factor (typically 10-15% better than equivalent AT-cut resonators).

The choice of which DRAT crystal cut to use is dependent upon a number of factors including the desired operating temperature. As can be seen from the frequency-temperature curves in Fig. 8, FC-cut, IT-cut and SC-cut crystals have widely different lower and upper turning point temperature and therefore the choice of crystal cut and oven temperatures should be closely coordinated. Typical turning point temperature ranges for the most popular cuts are provided in the following table. In addition, data are also provided for modified SC-cuts (i.e. SCM1 and SCM2) which are preferred for higher oven temperatures. It should be noted that the nominal C_1 values for the SCM2 cuts are approximately 10% lower than for regular SC-cuts.

Type Of Cut	Turning Point	Typical Turning Point Temperature Range
FC	Upper	+ 55°C to + 75°C
IT	Upper	+ 85°C to + 105°C
SC	Lower	+ 60°C to + 80°C
SCM1	Lower	+ 65°C to + 85°C
SCM2	Lower	+ 85°C to + 100°C

For your specific requirements consult our engineering staff.

5. Encapsulation, Resistance Welding Technique

The quartz vibrator is mounted in a low loss holder system (Fig. 9) in order to obtain high Q.

Electrical energy is applied to the resonator via the mounting and the thin, evaporated electrodes.

For higher mechanical demands, in particular shock and vibration resistance, special installation styles with three or four point fixing have been developed (Fig. 10). For the highest demands, i.e. mechanical resistance, the oscillator crystal housing HC-35/U is particularly suitable, whereby the vibrator disc is mounted on up to four points, 'lying', that is, parallel to the base plate.

Thereby, it is possible to survive extreme peak accelerations up to 18.000 g.

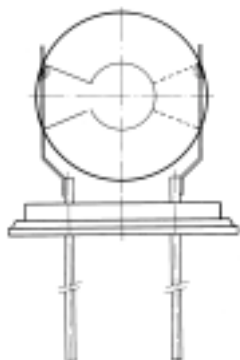


Fig. 9: Low Loss Holder System

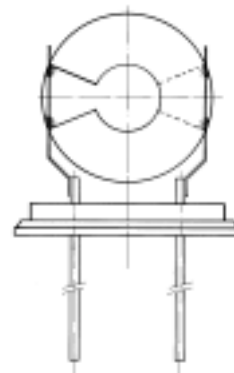


Fig. 10: Low Loss Holder System For Higher Mechanical Demands

The quartz vibrator is protected from outside influences in a hermetically sealed casing, either filled with protective gas or evacuated. A precondition for a low ageing rate is a maximum cleanliness of the protective gas and the inner housing, as well as an impeccable hermetic seal. For that reason, sealing technique is of the utmost importance.

A technically simple type of sealing is by soldering together the housing can and base, however when soldering, fluxing agents and other gases released by the heating reach the inner casing and deteriorate the ageing characteristics of the crystal. This technique is therefore seldom used today.

A type of sealing not subject to these disadvantages is called resistance welding. In this case, can and base are pressed together and welded by means of a current impulse.

An all-glass housing (enclosure) is used for applications requiring maximum aging stability (precision oscillators). For these, the blank vibrator is sealed under vacuum by fusing the glass base and the glass cap.

For individual frequency ranges and for different applications, several casing types are standardized, defined by the national standard bodies (IEC, DIN, BS, MIL, etc) and there are different designations for identical enclosures. In general, the MIL-designations have prevailed in practical use and we use these in our specification sheets. For details please have a look on our enclosure overview.

6. Equivalent Circuit And Motional Parameters

The electrical properties of the oscillator crystal as a function of the frequency can be depicted in the vicinity of the resonance frequency by an equivalent circuit diagram (Fig. 11). (compare IEC-Public. 122-2). The oscillating mass is symbolized by the dynamic inductance L_1 , whereas the elasticity is represented by the dynamic capacitance C_1 .

Overtone resonances, as well as spurious resonances can be depicted by additional, parallel connected series resonance circuits. At higher frequencies (above 100 MHz), a parallel conductance value G_0 may be required for modelling the behaviour. The insulation resistance is also modelled in this. The insulation resistance may be impaired by the following influences:

1. Fine leak of the glass feedthrough due to insufficient glass quality.
2. Long-term effect: through the migration of electrode material (silver) along so-called etching channels which can form due to non-homogenities in the crystal growth. This migration can only occur when a DC voltage is applied between the crystal pins over an extended period (several years) and has so far only been observed occasionally. The insulation resistance can collapse down to a few k Ω . the result of this is that the DC operating point of the capacitance diode connected to the capacitance diode connected to the crystal is displaced in VCXO circuits, which in turn leads to a greater frequency shift occurring.

It is therefore recommended to operate quartz crystals free of DC voltage by connecting a blocking capacitor (a few nF) in series to the crystal unit.

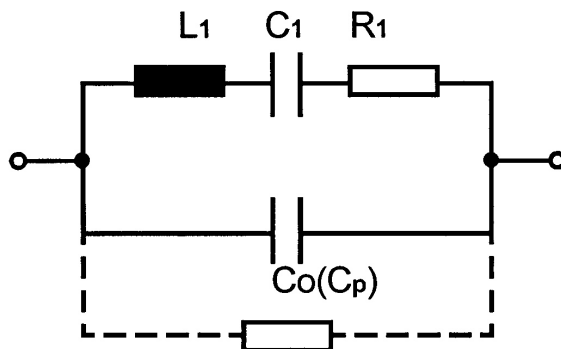


Fig. 11: Equivalent Circuit Diagram

In addition, a parallel capacitance C_p which differs from the static capacitance C_0 measurable at low frequencies acts at high frequencies owing to the influences of the lead and leakage reactances.

The value of the dynamic capacitance C_1 is very small in comparison with capacitances normally found in oscillating circuits in telecommunications and is calculated for a plano parallel quartz disc as follows ($1 \text{ fF} = 10^{-15} \text{ F}$):

$$C_1 [\text{fF}] = 0,1 \cdot k_c \cdot d_{el}^2 [\text{mm}^2] \cdot \frac{f_s [\text{MHz}]}{n^3}$$

f_s = resonance frequency

d_{el} = electrode diameter

n = ordinal number of the harmonics (1, 3, 5, 7, 9 ...)

k_c = correction constant

$k = 1$ for fundamental oscillation

$k = 0.85$ for 3rd overtone

$k = 0.75$ for 5th and higher overtones

With a given resonance frequency it can be seen that the C_1 can be varied by changing the electrode diameter, this variation is limited by the actual diameter of the quartz vibrator.

For frequencies lower than 1.8 MHz in enclosures HC-48/U and HC-51/U, also below 6 MHz for enclosures HC-50/U and HC-49/U and also below 8.5 MHz in enclosures HC-35/U and HC-52/U, it is no longer practicable to use a plano parallel resonator as the losses introduced by the mounting system become intolerable. In these cases by using the grinding techniques of the optical industry either plano-convex or bi-convex resonators are employed.

This technique substantially reduces the values of C_1 (the dynamic capacitance) that are obtained when using a plano parallel resonator.

This is the reason for the non-linearity of the C_1 graph shown on our data sheets for fundamental resonators in these holder styles.

For fundamental frequencies above 20 MHz, the value of C_1 is limited by the unacceptable increase in superious resonances if the value of C_1 is increased above 30 fF.

L_1 and C_1 are related by Thomson's formula:

$$L_1 = \frac{1}{\omega_s^2 C_1}$$

The dynamic resistance of the crystal unit R_1 represents the mechanical losses due to molecular friction within the resonator plus the damping induced by the mounting system and the accoustical damping of the gasfilled housing. The static capacitance C_0 represents the capacitance between the evaporated electrodes using the quartz resonator material as the dielectric.

$$C_{0p} [pF] = 0,02 \cdot d_{el}^2 [mm^2] \cdot \frac{f_s [MHz]}{n}$$

Thus the capacitances of the mounting system and the casing have to be added (0.3 pF to 2 pF), which leads to a new equivalent circuit (as shown in Fig. 12).

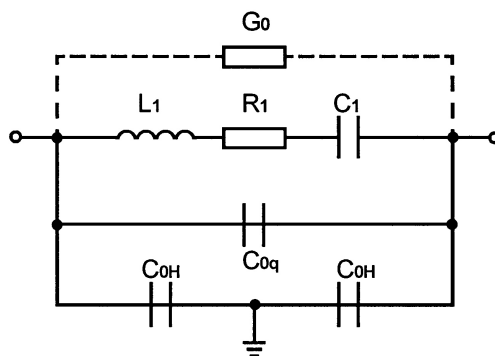


Fig. 12: New Equivalent Circuit Diagram

Depending on the particular enclosure type C_0 normally lies between 1 pF and 9 pF, oscillator crystals are normally designed with C_0 less than 7 pF. Its value can be influenced by an appropriate electrode diameter.

For exact measurement of C_0 it is essential to indicate if the measurement must be made with the crystal housing grounded or not. Likewise the frequency at which the measurement of C_0 is performed must be off the resonance frequency of the crystal to be measured (usually 1 MHz or between 10 MHz and 15 MHz). Measurement near to the resonance frequency indicates the parallel capacitance C_p which may differ from C_0 , particularly at high frequencies.

The quality Q of the quartz crystal units is specified as

$$Q = \frac{1}{2\pi f_s R_1 C_1} = \frac{2\pi f_s L_1}{R_1}$$

See the table below for typical practical values of Q .

Mode	Frequency Range			Quality/f [MHz]
	HC-51/U	HC-49/U	HC-35/U HC-52/U	
Fundamental mode		2.1 MHz – 2.5 MHz	4.0 MHz – 5.0 MHz	75.000 – 230.000
		2.5 Hz – 4.35 MHz	5.0 MHz – 8.0 MHz	230.000 – 450.000
	3 MHz – 8.5 MHz			330.000 – 500.000
		4.35 MHz – 11MHz	8 MHz – 12.5 MHz	400.000 – 600.000
	8.5 MHz – 55 MHz	11 MHz – 55 MHz	12.5 MHz – 53 MHz	100.000 – 400.000
3 rd overtone	15 MHz – 108 MHz	15 MHz – 120 MHz	20 MHz – 120 MHz	400.000 – 700.000
5 th , 7 th and 9 th overtone	30 MHz – 360 MHz	30 MHz – 360 MHz	30 MHz – 360 MHz	500.000 – 1.000.000

In Fig. 13, the curve of the reactance of a lossless crystal resonator is shown. There are two resonance frequencies, the series resonance frequency f_s and the resonance frequency f_p .

$$f_s = \frac{1}{2\pi\sqrt{L_1 C_1}} \quad f_p = \frac{1}{2\pi\sqrt{L_1 \frac{C_1 \cdot C_0}{C_1 + C_0}}} = f_s \sqrt{1 + \frac{C_1}{C_0}}$$

The series and parallel resonance frequencies are related by the formula:

$$\frac{f_p - f_s}{f_s} \approx \frac{1}{2} \cdot \frac{C_1}{C_0}$$

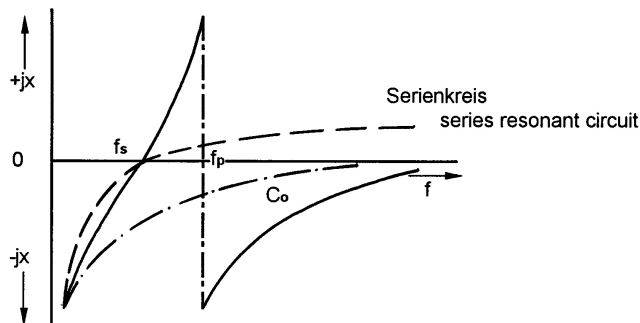


Fig. 13: Curve Of The Reactance Of A Lossless Crystal Resonator

However, for a "lossy" crystal the dynamic branch of the equivalent circuit comprises L_1 , C_1 and R_1 which are in parallel with C_0 . Thus the impedance of this combination is only real at the resonance frequency f_r above f_s .

Furthermore the complex impedance is given by:

$$Z_s = \frac{R_1 \cdot jX_0}{R_1 + jX_0} \quad \text{mit } X_0 = \frac{-1}{\omega C_0}$$

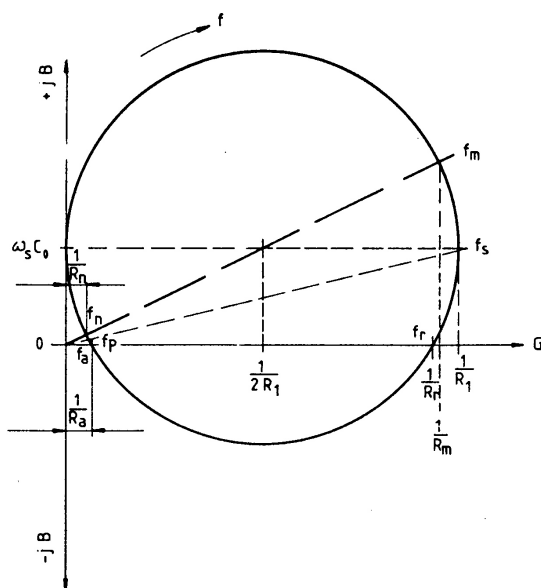
$$= \frac{R_1 X_0^2}{R_1^2 + X_0^2} + j \frac{R_1^2 X_0}{R_1^2 + X_0^2}$$

The phase angle at the series resonant frequency f_s is given by

$$\omega = \arctan\left(\frac{R_1}{X_0}\right) = \arctan(-R_1\omega C_0) = -\arctan R_1\omega C_0$$

The series resonant frequency of L_1 and C_1 is not the only frequency of the quartz crystal, as can be seen from the polar diagram (Fig. 14) representing the admittance of the circuit.

The most important frequency for practical application is the resonance frequency f_r at phase 0. The measurement technique in accordance with (DIN) IEC 444 also refers to this frequency. The frequencies f_a , f_p and f_n lying at the high-impedance end of the circle cannot be excited in oscillators. The centre of the circle is defined by the angle $\phi_M = \arctan(2 R_1 \omega C_0)$ and its distance from the real axis given by $B_0 = \omega C_0$.



- f_r : Resonanzfrequenz bei Phase 0
Resonance frequency with phase 0
- f_s : Serienresonanzfrequenz
Series resonance frequency
- f_m : Maximaladmittanz-(Minimalimpedanz-)Frequenz
Maximum admittance-(minimum impedance-) frequency
- f_a : Antiresonanzfrequenz (Phase 0)
anti(or negative) resonance frequency (phase 0)
- f_p : Parallelresonanzfrequenz (verlustfrei)
Parallel resonance frequency (loss-less)
- f_n : Minimaladmittanz-(Maximalimpedanz-)Frequenz
Minimum admittance-(maximum impedance-) frequency

Fig. 14: Polar Diagram

With increasing frequency the angle between the centre of the circle and the G-axis increases, thus the frequency differences between f_r , f_s and f_m also increase. Likewise the resistance R_r at zero phase also increases in comparison with R_1 . The so-called figure of merit

$$M = \frac{1}{\omega C_0 R_1}$$

shows on the diagram as the difference between f_r and f_s (or R_r and R_1). At frequencies above 120 MHz, M can become smaller than 2, so that the locus no longer cuts the G -axis, thus f_r disappears and is no longer seal.

7. Quartz Crystal With Load Capacitance C_L

Fundamental mode quartz crystals are normally operated with a load capacitance, which allows the circuit capacitance variations to be compensated. The load capacitance is normally in series or in parallel (Fig. 15 and 16) with the resonator and this causes it to oscillate at a new frequency, which sometimes is called "parallel resonance frequency", even though the load resonance frequency f_L should always lie far nearer the resonance frequency f_r (or f_s) than the parallel resonance frequency f_p and the load resonance resistance R_L which acts in this case is only slightly than R_r (or R_1) and far lower than R_p .

Overtone crystals in application without frequency modulation and FSK (Frequency Shift Keying) are often used at (series) resonance without load capacitance as the circuit normally contains a tuned (LC) circuit and the necessary compensation can be achieved by slightly detuning this element.

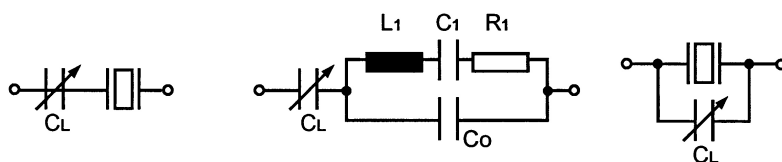


Fig. 15:
Crystal With Load Capacitance In Series

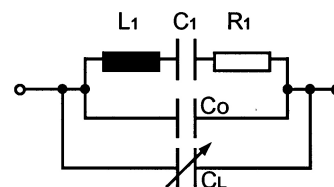


Fig. 16:
Crystal With Load Capacitance In Parallel

In Fig. 17 we show the reactance curves for a quartz crystal, then with a load capacitance in series and then in parallel with quartz resonator. In the two latter cases it can be seen that a new frequency is produced.

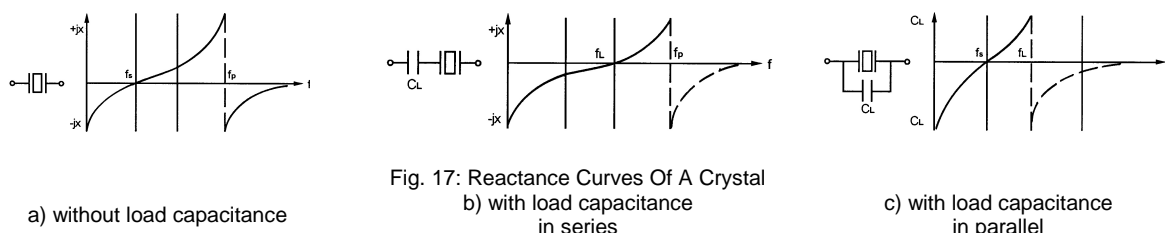


Fig. 17: Reactance Curves Of A Crystal

It can be seen that the difference between f_s and f_L is the same whether the capacitance is placed in series or in parallel with the crystal unit.

$$f_L = f_s \cdot \sqrt{1 + \frac{C_1}{C_0 + C_L}} \approx f_s \left(1 + \frac{C_1}{2(C_0 + C_L)} \right)$$

The resistance R_L with series load capacitor is naturally higher than R_1 .

$$R_L = R_1 \left(1 + \frac{C_0}{C_L} \right)^2$$

If one defines the difference in frequency between f_L and f_s as load resonance frequency offset D_L , then we have

$$D_L = \frac{f_L - f_s}{f_s} \approx \frac{C_1}{2 \cdot (C_0 + C_L)}$$

The pulling range of the element is defined as the change in frequency produced by changing the load capacity from one value to another (e.g. from maximum to minimum of a trimmer capacitor):

$$D_{L_1}, D_{L_2} = \frac{f_{L_1} - f_{L_2}}{f} \approx \frac{C_1 (C_{L_2} - C_{L_1})}{2 \cdot (C_0 + C_{L_1}) \cdot (C_0 + C_{L_2})}$$

Finally, we can define pulling sensitivity S as the frequency change in parts per million per pF change in the load capacitance:

$$S = \frac{1}{f_r} \cdot \frac{df_L}{dC_L} \approx - \frac{C_1}{2 \cdot (C_0 + C_L)^2}$$

From the above formula we can deduce:

With low value load capacitances, the change/pF would make S very large and thus the practical minimum value lies in the range between 8 and 10 pF. Conversely, with high load capacitances the pulling sensitivity is very small, so probably 100 pF represents, approximately, the upper limit.

The pulling sensitivity of the crystal unit can be considerably increased if the C_0 is compensated (see Fig. 18).

The formula for compensation is:

$$L_P = \frac{1}{\omega_r^2 \cdot C_0}$$

Which gives us:

$$f_L = f_s \cdot \sqrt{1 + \frac{C_1}{C_L}} \approx f_s \cdot \left(1 + \frac{C_1}{C_L}\right)$$

Thus the pulling range between the two values C_{L1} , and C_{L2} becomes

$$D_{L_2, L_1} \approx C_1 \frac{(C_{L_2} - C_{L_1})}{2 \cdot C_{L_1} \cdot C_{L_2}}$$

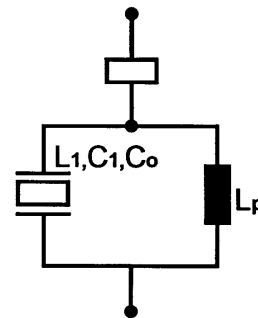


Fig. 18: C_0 Compensation

and the pulling sensitivity is

$$S = - \frac{C_1}{2 \cdot C_L^2}$$

There is another possibility to increase the pulling sensitivity and this is to replace the series load capacitor with a series tuned circuit comprising L_L , C_L when we have the new formula

$$f_L = f_s \cdot \left(1 + \frac{C_1}{2 \cdot \left(C_0 - \frac{1}{\omega_s^2 \cdot L_L - \frac{1}{C_L}} \right)} \right)$$

There is however a potential disadvantage to this method, the effective Q of the combination is dramatically reduced due to the relatively low Q of the inductance employed. Furthermore there is also an additional tuned circuit created, consisting of L_L , C_L and the C_0 of the quartz element, this potential parasitic frequency is not quartz controlled.

In practice it is very important to determine accurately the load capacitance or input capacitance of the circuit into which the quartz crystal is to be introduced, as the pulling sensitivity at $C_L = 30$ pF is about 10 ppm/pF.

This load capacitance is defined during the manufacture of the quartz crystal and in its operational circuit comprises the sum of whatever actual capacitances form the oscillator network plus the stray capacitances of wiring and adjacent semiconductor elements, as well as the phase changes introduced by the latter which have an effect, however small.

The most simple way to determine the load capacitance suitable for a particular circuit is to measure an operational frequency in the middle of the pulling range with an available crystal of approximately the correct frequency. This frequency is then transferred to a passive measuring network in the factory and the operational frequency reproduced by variations of the load capacity in the network, which can then be accurately determined.

Standard values of load capacitance in current use in the industry are 10, 12, 15, 20, 30 or 50 pF.

The current valid method of measuring load resonance frequencies is described in (DIN) IEC 444-4.

8. Measurement Of Quartz Crystal Parameters

There are basically two methods, normally called either active or passive.

In the active method the crystal unit is used in an oscillator as the frequency determining unit. These oscillators have become known in the industry as 'test sets' and have been developed to cover specific frequency ranges. In a test set the quartz crystal oscillates largely independently of its resonance resistance and its other parameters, C_1 , L_1 and C_0 . The resonance resistance is determined by the substitution of an equivalent resistor to obtain the same output level from the oscillator. The absolute measurement accuracy of a test set is generally considered to be between 10 and $15 \cdot 10^{-6}$. However, with careful adjustment and measurement this can be reduced to be $5 \cdot 10^{-6}$ between different test sets.

Today however, adjustment tolerances often are as low as 5 or $10 \cdot 10^{-6}$ and this then precludes the use of 'test sets' for measurement purposes.

The passive or Pi-network method according to IEC-publication 444-1, which claims an accuracy of at least ten times better, is nowadays in general usage.

For this reason, the frequency must be determined to within an accuracy of approximately $\approx 5 \cdot 10^{-7}$. This requirement is met with the passive measurement method in accordance with (DIN) IEC 444. The classic method taken from (DIN) IEC 444-1 (DIN) IEC 444-4 is described below.

8.1 Passive Measurement Up To 125 MHz According To IEC 444-1 and 444-2

The crystal is in a double Pi-network as shown in Fig. 19, which has the effect of isolating the crystal unit from the measuring devices.

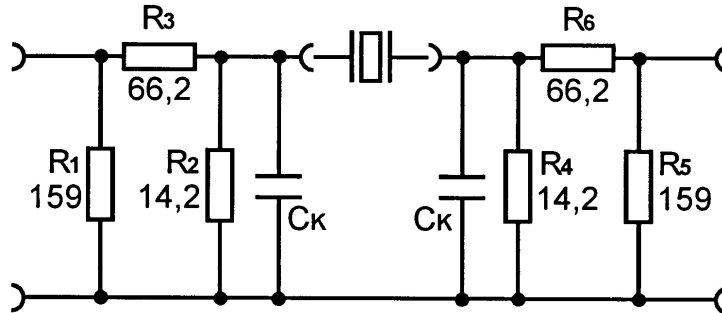


Fig. 19: Double Pi-Network

Seen from the crystal unit, the network impedance amounts to 12.5 ohms on both sides. It is therefore loaded with 25 ohms nominally.

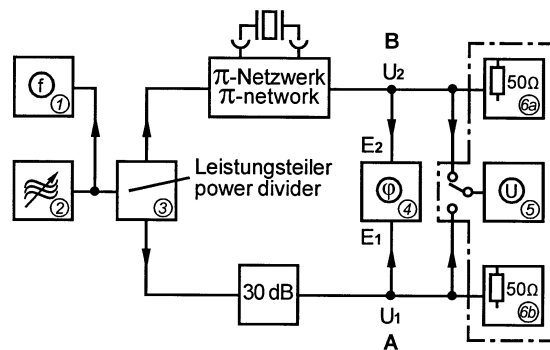


Fig. 20: Passive Measuring Arrangements

Figure 20 shows the measuring arrangements. The frequency generator or synthesizer (2) is tuned in to the frequency required, which shows phase 0 between the points 'A' and 'B', measured with a vector-voltmeter or network analyzer (3). The frequency is indicated by the frequency counter (1) and from the ratio of the voltages at points 'A' and 'B' we can calculate the resonance resistance of the crystal. By variation of the generator output level the desired level of drive can be applied.

It is possible to partially automate this process, the frequency of the generator being controlled by either analogue or digital methods, whereby the phase of the generator is locked to the crystal by means of the phase proportional output voltage of (4).

8.1.1 Measurement Of The Resonance Frequency f_r And Resistance R_r

The measurement at zero phase gives the resonant frequency f_r , which is higher than the series resonance frequency f_s determined by the L_1 and C_1 (see Fig. 14) and we have

$$\frac{f_r - f_s}{f_s} = \frac{1}{2 \cdot Q} \arctan(R_1 \cdot \omega \cdot C_0)$$

For small phase angles the relationship may be simplified to

$$\frac{f_r - f_s}{f_s} \approx \frac{C_0}{C_1 \cdot 2 \cdot Q^2} = \frac{r}{2 \cdot Q^2}$$

$$r \dots \text{capacitance ratio} \frac{C_0}{C_1}$$

$$Q \dots \text{quality factor}$$

The capacitance ratio C_0/C_1 is about 220 for AT-cut fundamental resonators, 2400 for 3rd overtone and 7500 for 5th overtone. A deviation of $\pm 5 \cdot 10^{-7} = \pm 0.5$ ppm is achieved at 125 MHz with a 5th harmonic crystal and $Q = 80000$. For higher frequencies or overtones an exact measurement is only possible where the C_0 has been compensated (see 8.2).

Manufacturer and user must agree, if measurements are to be made in these higher frequency ranges with the static capacity C_0 either compensated or uncompensated, as variations of up to 20 ppm will be seen, dependent on the frequency being measured and the Q of the resonator.

The measurement of the resonance R_r is carried out in the following way:

1. A short circuit is placed in the measurement head and the voltage U_{BK} is measured at 'B' (Fig. 20).
2. The crystal replaces the short circuit and the voltage U_B is measured at point 'B' at phase zero.

With phase zero between the input and the output of the measuring head (points 'A' and 'B') we then have

$$R_r = 25\Omega \cdot \left(k \cdot \frac{U_{BK}}{U_B} - 1 \right)$$

$$\text{whereby } k = \frac{U_A}{U_{AK}} \approx 1$$

For example, where the resonance resistance is approximately 25 ohms it is possible to calculate the drive level adjusting the U_{BK} level in accordance with the relationship.

$$U_{BK}(mV) = 57,8 \sqrt{P_c(mW)}$$

$$U_{BK}(mV)L = 9,14 \cdot I_c(mA)$$

We obtain the following for other values of R_r :

$$U_{BK}(mV) = 5,18 \cdot (R_r(\Omega) + 25\Omega) \sqrt{\frac{P_c(mW)}{R_r(\Omega)}}$$

$$U_{BK}(mV) = 0,183 \cdot I_c(mA) \cdot (R_r(\Omega) + 25\Omega)$$

At the resonance frequency f_r , the actual values of the drive level can be calculated directly from the U_B level:

$$P_c(\mu W) = 0,048 \cdot R_r(\Omega) \cdot U_B^2(mV^2)$$

$$I_c(mA) = \frac{U_B(mV)}{4,57}$$

8.1.2 Measurement Of Parameters C_1 And L_1

The dynamic capacitance and inductance of the quartz crystal can be determined in several different ways.

A method giving limited accuracy for frequencies below 30 MHz is outlined in IEC 302 and utilises the change of frequency with two different load capacities.

For exact measurement and above 30 MHz the phase offset method described below should be used as outlined in IEC 444-2 or the so-called circle method in accordance with (DIN) IEC 444-5, see 7.2

Phase Offset Method

As previously indicated one measures resonance resistance R_r at phase zero. The generator frequency is now adjusted in such a way that a phase difference of $+\varphi$ and $-\varphi$ is provided. From the frequency $\Delta f_{\pm\varphi}$ we can derive:

$$C_1 = \frac{\Delta f_{\pm\varphi}}{(2\pi f)^2 \cdot R_{eff} \cdot \tan \varphi}$$

but because of the Pi-network impedance of 25 ohms, then:

$$R_{eff} = R_r + R_T = R_r + 25 \Omega$$

We have

$$L_1 = \frac{R_{eff}}{(2\pi X \Delta f_{\pm\varphi})} \cdot \tan \varphi$$

and for Q

$$Q = \frac{\omega_r L_r}{R_r} = \frac{1}{\omega_r C_1 R_1}$$

With phase offsets of 45° , the value of $\tan 45^\circ = 1$ and the formula are simplified.

The formula are only valid if the value of C_0 is ignored. Figure 21 gives a graphical illustration of the measurement error of C_1 depending on the figure of merit M with respect to the phase offset.

$$M = \frac{1}{\omega_r C_0 R_r}$$

as parameter.

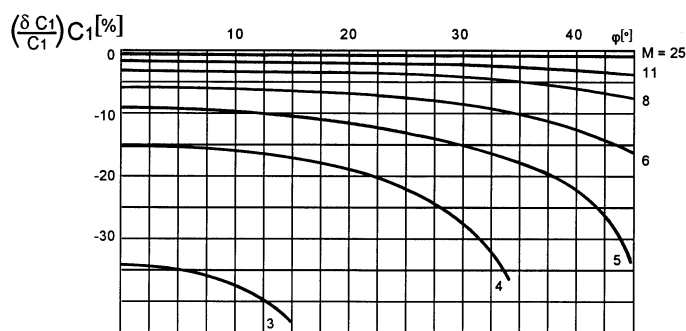


Fig. 21: Phase Offset

8.2 Measurement In Accordance With The Circle Method (DIN) IEC 444-5 Up To 500 MHz.

The above-described method in accordance with (DIN) IEC 444-2 is, to an ever-increasing extent, being superseded by a new, more precise method in accordance with (DIN) IEC 444-5 which we term the „circle method“. Error correction is carried out by complex modelling of the Pi section, with the same measuring set-up as in Figures 11 + 12, and on the basis of extended calibration with short-circuit no-load state and calibration resistor.

The measurement points do not necessarily lie exactly at the resonance frequency f_r or f_s but are suitably distributed on the admittance circle. The new version of (DIN) IEC 444-5 describes several software algorithms for computing the dynamic equivalent parameters from the complex impedance values of the crystal determined at the measuring frequency. This method is not restricted to measurements of amplitude and phase with the Pi section but can also be applied to S parameter test sets.

Method:

8.2.1 Calibration

Calibration with short circuit, measurement of the output voltage of the B channel.

$$\underline{U}_{BK} = \underline{U}_{BK} / \varphi_{BK}$$

Calibration with calibration resistor $\underline{R}_N = R_e(\underline{R}_N) + j\text{Im}(\underline{R}_N)$ results in

$$\underline{R}_N = \left(\frac{\underline{U}_{BK}}{\underline{U}_{BN}} - 1 \right) \cdot \underline{RT}$$

Measurement of an unknown impedance $\underline{R}_X = R_e(\underline{R}_X) + j\text{Im}(\underline{R}_X)$ at a measurement frequency f_x results in

$$\underline{R}_X = \left(\frac{\underline{U}_{BK}}{\underline{U}_{BX}} - 1 \right) \cdot \underline{RT}$$

R_x can be determined from this by

$$R_X = R_N \frac{\frac{\underline{U}_{BK}}{\underline{U}_{BX}} - 1}{\frac{\underline{U}_{BK}}{\underline{U}_{BN}} - 1}$$

The crosstalk capacitance C_c (crosstalk impedance R_{Cc}) can be determined with the above formula and calibration at no load, whereby \underline{U}_{BX} is substituted by the channel output voltage at no load $\underline{U}_{BL} = \underline{U}_{BL} / \varphi_{BL}$. C_c can be calculated as follows from the imaginary component of $\underline{R}_X = \underline{R}_{Cc}$ thus calculated

$$C_c = \frac{1}{2\pi f_c \cdot \text{Im}(\underline{R}_{Cc})}$$

8.2.2 Measurement Of The Crystal Parameters

1.) Measurement Of The Capacitance C_0 , C_p

Besides the static capacitance C_0 which is measured at 1 MHz with a capacitance bridge, this method can be used to determine the parallel capacitance C_p acting at the crystal frequency.

The crystal is connected into the Ri section and the complex voltage U_{BC} is measured at frequency f_c . C_p then results from the imaginary component of the measured impedance, as follows:

$$C_p = \frac{\frac{U_{BK}}{U_{BN}} - 1}{\left(\frac{U_{BK}}{U_{BC}} - 1 \right) \cdot j\omega R_N} - C$$

2.) Measurement Of The Characteristic Frequencies And The Dynamic Parameters

The method described in 7.2.1 involves determining the crystal impedance at two frequencies ω_1 and ω_2 and representing the values as admittance values:

$$\underline{Y}_1 = \frac{1}{\underline{R}_x}(\omega_1) = a_1 + jb_1$$

$$\underline{Y}_2 = \frac{1}{\underline{R}_x}(\omega_2) = a_2 + jb_2$$

From these, it is possible to calculate the dynamic crystal parameters explicitly as follows:

$$L_1 = \frac{\omega_1 \cdot b_1^* - \omega_2 \cdot b_2^*}{\omega_1^2 - \omega_2^2}$$

$$C_1 = \frac{\omega_1^2 - \omega_2^2}{\omega_2^2 \omega_1 b_1^* - \omega_1^2 \omega_2 b_2^*}$$

$$R_1 = \frac{a_1 + a_2}{2}$$

$$\text{with } a_j^* + jb_j^* = \frac{1}{a_j + j(b_j - \omega_j(C_0 + C_C))}$$

Even if the position of the measuring frequencies ω_1 and ω_2 is unfavourable, the series resonance frequency calculated from L_1 and C_1 is given by:

$$f_s = \frac{1}{2\pi\sqrt{L_1 \cdot C_1}}$$

on the basis of this, other, more favourable measuring frequencies can be determined if necessary. The optimum measuring frequencies lie at around $\pm 45^\circ$ referred to point f_s , i.e. at the „top“ and „bottom“ point of the circle.

Alternatively, it is also possible to approximately determine f_s by sweeping quickly „to positive“ and then „to negative“ in the anticipated frequency range and taking the mean value of the resultant maximum admittance frequency as the starting value for f_s .

The measuring method described above can be used up to frequencies of 500 MHz and above. It has been verified at IEC TC 49 up to 900 MHz and above. Please refer to the special TQ publication for further details.

The measurement technique is not restricted to a measurement technique of amplitude and phase with the Pi section but can also be used on S parameter test sets with error correction. See (DIN) IEC 444-5 for details.

The method for measurement of crystals above 125 MHz to 200 MHz with the aid of physical C_0 compensation, described in IEC 444-3, is thus rendered obsolete with the above-described method and is no longer state-of-the-art.

8.3 Measurement Of The Load Resonance (DIN) IEC 444-4

To date, the measurement of the load resonance f_L with the load resonance resistance R_L and the associated parameters of load resonance frequency offset D_L , pulling range $D_{L1,L2}$ and pulling sensitivity S has generally been conducted in the Pi section using a load C adaptor in accordance with (DIN) IEC 444-4.

The resultant measuring errors are far higher than when measuring f_r and R_r . A special publication provides an analysis of the measurement errors. Thus, TELE QUARZ now uses a modern method without load C adaptor. The load resonance frequency is determined by software in the normal Pi measuring head. An iterative search method determines the frequency f_L at which the crystal has a complex impedance given by the load capacitance.

$$Z_L = R_L + jX_L \quad \text{with} \quad X_L = \frac{1}{\omega C_L}$$

$$R_L = R_1 \left(1 + \frac{C_0}{C_L} \right)^2$$

Since (below 30 MHz in particular), the value of X_L is far higher than R_L , the frequency is determined at which the crystal impedance indicates the imaginary part X_L . The impedance is calculated as in Section 7.2.1 (circle method).

Particular care must be taken to ensure that the correct crystal load is allowed for.

This method has been verified by extensive comparison measurements. It provides an improvement by a factor of 3 to 5 in accuracy and reproducibility as compared with the adaptor method. This method is currently under preparation at IEC. Further details are to be described in a special publication.

9. Spurious Resonances

All quartz crystals have spurious resonances (unwanted resonance responses) besides the main resonance frequency. They are represented in the equivalent circuit diagram (Fig. 11 + 12) by additional resonant circuits in parallel with R_1 , L_1 , C_1 .

The ratio of spurious resonance resistance R_{NW} to resonance resistance R_r of the main wave is generally specified in the attenuation constant dB and is designated spurious attenuation a_{NW} :

$$a_{NW} = 20 \cdot \lg \frac{R_{NW}}{R_r}$$

For oscillator crystals 3 to 6 dB are normally sufficient. For filter crystals attenuations greater than 40 dB are often required. This can only be achieved by special design techniques and involves the use of very small values of the dynamic capacity C_1 .

The achievable attenuation decreases with higher frequency and with higher orders of overtone. It is found generally that plano-parallel quartz resonators have better spurious attenuation than plano-convex or bi-convex resonators. In specifying spurious resonance parameters it is necessary to give an indication of both the acceptable attenuation level desired and their frequencies relative to the main resonance frequency.

In the AT-cut the (so-called) 'unharmonic resonances' exist only above the main resonance in the region of + 40 to + 150 kHz for plano parallel resonators between + 200 to + 400 kHz for biconvex or planoconvex resonators.

In the passive measurement method indicated above, spurious resonance attenuations up to 20 to 30 dB can be measured. With higher attenuations, C_0 compensation is necessary.

The usual method, as specified in DIN 45 105, part 4/1 IEC publ. 283, utilizes the method with hybrid coils which because of insufficient specification does not produce reproducible results.

It is somewhat better and more reproducible to use a 180° hybrid power divider in place of the hybrid coil in accordance with Fig. 21.

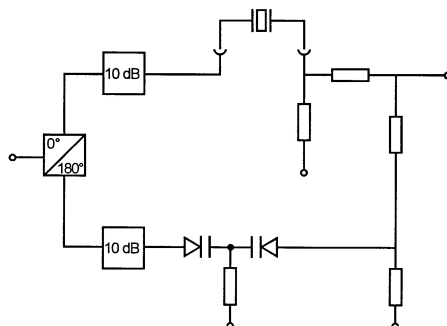


Fig. 21: 180° Hybrid Power Divider

Using the above-described circle method in accordance with (DIN) IEC 444-5 permits precise determination of the spurious resonances. Standardization for this is currently in preparation.

10. Drive Level (DLD)

The amplitude of mechanical vibration of the quartz resonator increases proportionally to the amplitude of the applied current. The power dissipated in the resonance resistance is given by

$$P_c = I_q^2 R_1$$

High drive levels lead to the destruction of the resonator or the vaporisation of the evaporated electrodes. The upper limit for drive level is approximately 10 mW.

As the reactive power oscillating between L_1 and C_1 is represented by $Q_c = Q \cdot P_c$, for $P_c = 1$ mW and with a Q of 100.000, Q_c is equal to 100 Watts. The oscillation amplitude can be exceeded with relatively low level of drive P_c , thus resulting in the crystal frequency moving upwards.

This frequency dependence on drive level is more pronounced with increasing overtone order. Figure 22 shows typical effects but exact prediction of the effect is not possible as it is influenced by all the elements of crystal design and operation i.e. Mechanical blank parameters, electrode size, mounting arrangements and so on.

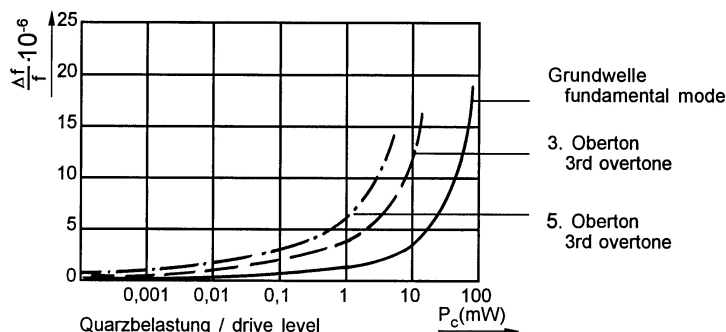


Fig. 22: Drive Level Dependence (DLD)

It can be seen that the drive level must be specified carefully, if there is to be good correlation between the frequency of the crystal at the end of its production and in the end use equipment.

Today with semiconductor oscillator circuits a drive level of approximately 0.1 mW appears normal, where this parameter is not specified, our production will use 0.1 mW.

A well performing crystal should start to oscillate easily and its frequency should be virtually independent of the variation of drive level from a starting level of about 1 nW. In today's semi-conductor circuits with very low power consumption the crystal has to work well also at very low drive levels.

In Fig. 23 we show the effect of crystals with and without the problem of frequency dependence on drive level. Crystals with badly adhering electrodes or on which the surface of the resonator is not fine enough, exhibit the curved effect i.e. at low drive levels they have higher resistance.

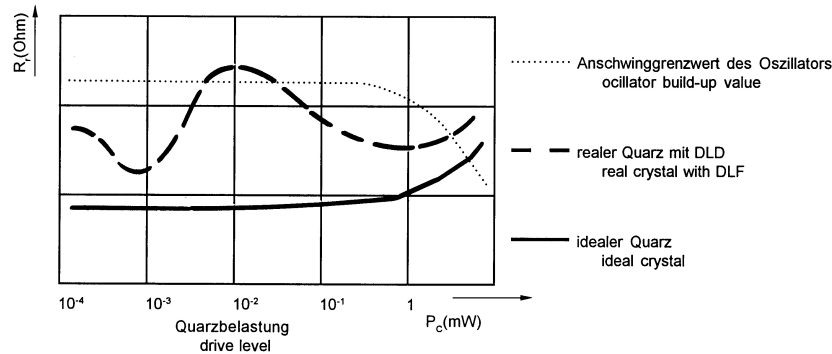


Fig. 23: Drive Level Dependence Versus Resonance Resistance

This effect is called the drive level dependence (DLD). Usually production tests of DLD are performed between 1 and 10 microwatts and then at 1 mW and again at a low load. The relative change in resistance is then used as the test criterion. Needless to say, making more measurements at intermediate levels increases crystal production costs considerably. Using suitable test oscillators permits fast testing of the DLD limit value, but only in the form of a Go/No-go test. IEC Draft 248 covers measurement of the drive level dependence of the resonance impedance with a passive measurement technique in accordance with (DIN) IEC 444-6 describes measurement of the drive level dependence of the resonance impedance with a passive measurement technique and with the oscillator method. Oscillation build-up problems can very largely be eliminated by optimizing the oscillator circuit by providing a sufficient feedback reserve and a „hard“ switch-on pulse.

11. Frequency Variation As A Function Of Time

This is normally considered in two ways. Short term stability (i.e. in the range of up to 10 seconds) and long term stability over days, months or years, often called ageing.

The short term stability of a quartz crystal depends on the actual oscillator design and manufacture. Only at low drive levels the short term stability of the oscillator is totally controlled by the quartz crystal.

The ageing rate is substantially influenced by the cleanliness of the resonator, the stability of the inert gas filling and the security of the final sealing process. Ageing is naturally greater during the first part of the life of the crystal unit.

$$\frac{\Delta f}{f} = a_0 + a_1 \cdot \lg(a_2 t + 1)$$

The frequency ageing can often be described by a logarithmic function of the form (see Figure 24).

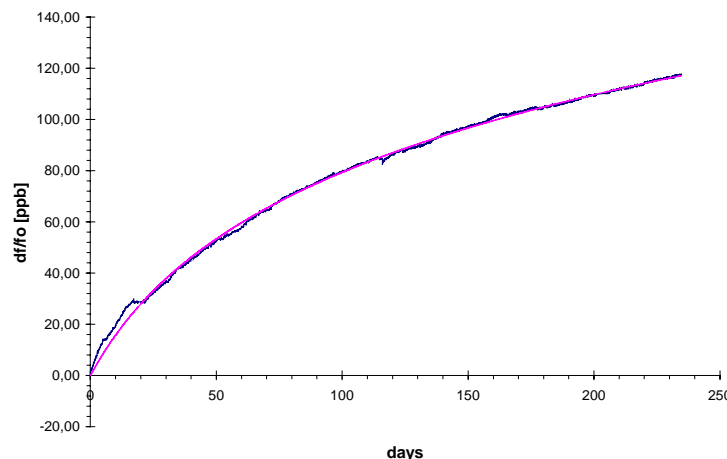


Fig. 24: Frequency Stability

It is necessary to distinguish between active and passive ageing. Active ageing is the frequency shift, when the crystal works under operation conditions, i.e. permanently oscillating in the circuit. Passive ageing is the frequency shift during storage. For accelerated ageing storage can be accomplished at elevated temperatures, e.g. 85° C.

Ageing rate is only meaningful if defined either as 'in operation' and under defined drive and temperature conditions i.e. active, or in storage under defined temperature conditions i.e. passive.

Ageing rates of less than 2 ppm per year are normal for crystals sealed in metal holders, in special cases 0.5 ppm per year is possible. As small as possible a load (10 µW) should be applied on the crystal for low ageing. On the other hand, as high as possible a load (several 100 µW) should be applied on the crystal for high short-term stability and low phase noise.

12. Information On Processing

Oscillator crystals have an hermetically sealed housing (enclosure) which is filled with inert gas or evacuated. If an oscillator crystal has a leak, thus permitting normal atmosphere to penetrate it, this may result in serious deviations in the crystal data. The following information relates to possible problems in processing which may lead to leaks.

12.1 Glass Leadthroughs

The most sensitive point on the oscillator crystal is the glass leadthrough. Damage may occur as the result of mechanical overload, such as bending the connection leads for horizontal mounting. In order to avoid microcracking, the wire must be held fixed in position by a pressure pad between glass leadthrough and the bending point during the bending process.

Check: there should be no damaged edges on the glass leadthrough after bending.

The center spacing of the PC board must correspond to the crystal center spacing.

HC-49/U enclosure: 4.9 mm center spacing

HC-52/U enclosure: 3.75 mm center spacing

Tolerance: ± 0.2 mm

If crystals are to be mounted vertically, the base of the crystal should contact the PC board flat. If there is a space between the PC board and the crystal this may result in fatigue fractures of the connection leads or damage to the glass leadthroughs if subject to vibration movements.

12.2 Soldering

Crystals can be processed using conventional soldering processes such as wave soldering, convection, infrared, and vapour phase reflow soldering under normal conditions. Test conditions for solderability, resistance to dissolution of metallization and to soldering heat see table below (page 21).

Solderability is guaranteed for one year storage under normal climatic conditions (+5°C to +35°C @ 40% to 75% relative humidity), however typically sufficient solderability –depending on the process – is maintained also for longer time periods. In cases of doubt, components older than one year should undergo a sample solderability test.

Applicable reflow soldering profiles for SMT components are as in IEC 61760-1 (Fig. 25). For temperature profiles with higher thermal stress, such as for lead-free solder processes, please contact the manufacturer.

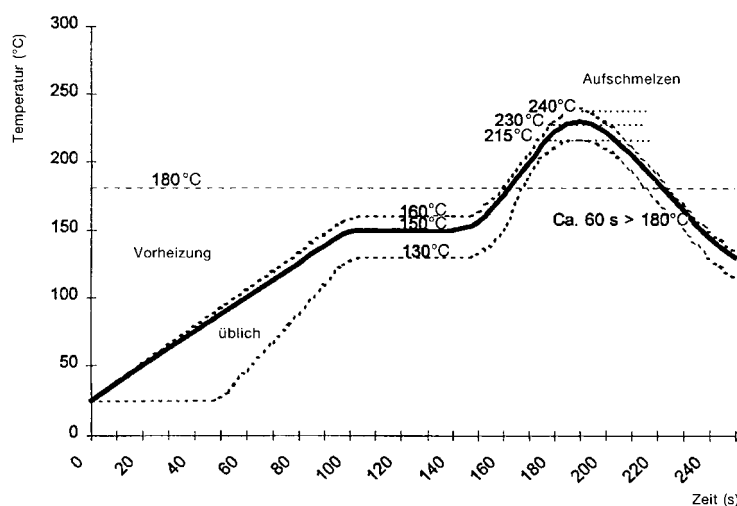


Fig. 25: Recommended IR and Convection Reflow Soldering Temperature Profile
source: IEC 61760-1

After reflow soldering the frequency of the products may have shifted several ppm, which relaxes after several hours or days, depending on the products (see ref.: BNeubig[1]). For details please contact the manufacturer.

12.3 Cleaning

Our crystals can be processed using conventional cleaning processes under normal conditions. However, this may be limited to a greater or lesser extent, dependent upon type and tolerance. In cases of doubt, please consult us.

Ultrasonic cleaning is not harmful to crystals at ultrasonic frequencies of 20 kHz at the sound intensities conventional in industry. Sensitive crystals may suffer mechanical damage of the crystal wafer if subjected to 40 kHz ultrasonic baths and high sound pressure. In cases of doubt, please conduct tests under practical conditions with crystals which have been mounted on the PC board.

12.4 Application

Unless otherwise noted, the products listed in the catalogue are designed for use with ordinary electrical devices, such as stationary and portable communication, control, measurement equipment etc.. They are designed and manufactured to meet a high degree of reliability (lifetime more than 15 years) under normal „commercial“ application conditions.

Products dedicated for automotive and H-Rel applications are specifically identified for these applications. If you intend to use these „commercial“ products for airborne, space or critical transport applications, nuclear power control, medical devices with a direct impact on human life, or other applications which require an exceptionally high degree of reliability or safety, please contact the manufacturer.

12.5 Tape & Reel

The packing in tape & reel is according to IEC 60286-3.
Details see Tape & Reel data sheets.

12.6 Qualification

We provide regular qualification tests on our standard product range. Results are available upon request. Customer specific qualification tests are subject to agreement.

If not otherwise stated, the product qualifications are performed according to IEC 61178-3.

12.7 Mechanical & Climatic Tests

If not otherwise stated the products withstand the tests listed in the following table (page 21) in accordance with IEC 61178-1, which are based on IEC 60068-2. Tests to other standards such as MIL-PRF-55310, MIL-STD 883, ETSI, ITU etc. upon request.

Recommended Environmental Test Conditions

Test	IEC 60068 Part ...	IEC 61178-1 clause ...	Test conditions
Visual inspection, dimensions		4.5 4.6	Enclosure styles as in IEC 60122-3, if applicable
Robustness of terminations	2-21	4.8.1	Tests Ua1, Ua2, Ub
Sealing tests	2-17	4.8.2	Gross leak: Test Qc, Fine leak: Test Qk
Solderability Resistance to soldering heat	2-20	4.8.3	Test Ta (235 ± 5)°C Method 1 Test Tb Method 1A, 5s
Shock	2-27	4.8.8	Test Ea, 3 x per axes 100g, 6 ms half-sine pulse
Bump	2-29	4.8.6	Test Eb, 4000 bumps per Axes, 40g, 6 ms
Free fall	2-32	4.8.9	Test Ed procedure 1, 2 drops from 1m height
Vibration, sinusoidal	2-6	4.8.7	Test Fc, 30 min per axes, 10 Hz - 55 Hz 0,75mm; 55 Hz - 2 kHz, 10g
Vibration, random	2-36	4.8.7	Test Fdb
Rapid change of temperature	2-14	4.8.5	Test Na, 10 cycles at extremes of operating temperature range
Dry heat	2-2	4.8.11	Test Ba, 16 h at upper temperature indicated by climatic category
Damp heat, cyclic	2-30	4.8.12	Test Db variant 1 severity b), 55°C/95% r.H., 6 cycles
Cold	2-1	4.8.13	Test Aa, 2 h at lower temperature indicated by climatic category
Climatic sequence	1-7	4.8.14	Sequence of 4.8.11, 4.8.12 (1 st cycle), 4.8.13, 4.8.12 (5 cycles)
Damp heat, steady state	2-3	4.8.15	Test Ca, 56 days
Immersion in cleaning solvents	2-45 2-70	4.8.16	Test Xa for superficial marking only
Endurance tests - ageing - extended aging		4.9.1 4.9.2	30 days @ 85°C 1000h, 2000h, 8000h @85°C